Low Temperature Plasma-Enhanced Atomic Layer Deposition of Metal Oxide Thin Films

S. E. Potts, W. Keuning, E. Langereis, G. Dingemans, M. C. M. van de Sanden and W. M. M. Kessels

J. Electrochem. Soc. 2010, Volume 157, Issue 7, Pages P66-P74.
doi: 10.1149/1.3428705

Journal of The Electrochemical Society, **157** (7) P66-P74 (2010)
0013-4651/2010/157(7)/P66/9/$28.00 © The Electrochemical Society

Low Temperature Plasma-Enhanced Atomic Layer Deposition of Metal Oxide Thin Films

S. E. Potts,[*,z] W. Keuning, E. Langereis,[*] G. Dingemans, M. C. M. van de Sanden, and W. M. M. Kessels[*,z]

Department of Applied Physics, Eindhoven University of Technology, 5600 MB Eindhoven, The Netherlands

Many reported atomic layer deposition (ALD) processes are carried out at elevated temperatures (>150°C), which can be problematic for temperature-sensitive substrates. Plasma-enhanced ALD routes may provide a solution, as the ALD temperature window can, in theory, be extended to lower deposition temperatures due to the reactive nature of the plasma. As such, the plasma-enhanced ALD of Al_2O_3, TiO_2, and Ta_2O_5 has been investigated at 25–400°C using $[Al(CH_3)_3]$, $[Ti(O^iPr)_4]$, $[Ti(Cp^{Me})(O^iPr)_3]$, $[TiCp^*(OMe)_3]$, and $[Ta(NMe_2)_5]$ as precursors. An O_2 plasma was employed as the oxygen source in each case. We have demonstrated metal oxide thin-film deposition at temperatures as low as room temperature and compared the results with corresponding thermal ALD routes to the same materials. The composition of the films was determined by Rutherford backscattering spectroscopy. Analysis of the growth per cycle data and the metal atoms deposited per cycle revealed that the growth per cycle is strongly dependent on the film density at low deposition temperatures. Comparison of these data for Al_2O_3 ALD processes in particular, showed that the number of Al atoms deposited per cycle was consistently high down to room temperature for the plasma-enhanced process but dropped for the thermal process at substrate temperatures lower than 250°C.
 [DOI: 10.1149/1.3428705]

Manuscript submitted January 18, 2010; revised manuscript received April 16, 2010. Published May 14, 2010. This was Paper 2034 presented at the Vienna, Austria, Meeting of the Society, October 4–9, 2009.

Atomic layer deposition (ALD), a method of ultrathin-film deposition by alternate dosing of gaseous precursors, gives dense, pure, and highly conformal films with excellent step coverage. Each ALD process is considered to have a temperature window, which is governed by the reactivity and stability of the precursors and surface functional groups.[1] The ALD temperature window typically spans 200–400°C for the majority of processes, although many studies on metal oxides have been investigated over the range 100–600°C.[2] It is often assumed that, within the temperature window, a submonolayer of material is deposited during each cycle and that the growth per cycle remains constant with varying substrate temperature (Fig. 1a). However, in several cases it is possible to see a small reduction in the growth per cycle with increasing temperature due to a small loss of reactive surface groups (Fig. 1b).[3] Outside the temperature window, the growth per cycle can change dramatically. At lower temperatures, excess condensation of the precursors can result in a rapid increase in growth (A), for example, when the substrate temperature is lower than the bubbler temperature required to obtain an adequate vapor pressure. Also at lower temperatures, there may be insufficient thermal energy for a chemical reaction to occur, resulting in slower growth (B). At higher temperatures, decomposition of the precursors (chemical vapor deposition) can occur, leading to an increase in growth, which is not self-limiting (C), or, if the film material is volatile it may evaporate, thereby reducing the growth (D). However, as previously mentioned, a change in growth per cycle does not always accurately indicate whether or not true ALD is occurring, exemplified by the gradual loss of surface groups with increasing substrate temperature in Fig. 1b.

Generally, the ALD window (spanning 150–400°C) for most metal oxide processes has proved sufficient for many applications requiring ultrathin films. However, for emerging applications employing temperature-sensitive substrates, even temperatures as low as 200°C can be problematic, for example, in polymers or small organic molecules, whose structure can be affected at such temperatures. Applications that require such low temperatures include organic light emitting diodes for display and lighting applications,[4-8] in ZnO-based thin film transistors for (flexible) displays,[9,10] and in double patterning lithography where SiO_2 is deposited on a temperature-sensitive photoresist.[11] Such devices may require a moisture permeation barrier to prevent degradation, and aluminum oxide deposited by ALD is a popular choice. Another application requiring low deposition temperatures is the ALD of corrosion-resistant barrier layers, which can be applied to metal substrates.[12-14] For such substrates, overheating may cause surface oxidation, which may weaken the protective layer or change the substrates' mechanical properties. This can be problematic as corrosion-resistant applications require dense films with no defects. Generally, substrate temperatures ≤150°C are required, although these have not been widely reported so far for ALD. However, examples are known, which are summarized in Table I.

Despite the low temperature requirement, it is a generalization that the lower the substrate temperature, the higher the concentration of impurities. Examples of possible impurities include hydroxyl groups and carbon in Al_2O_3 processes[6,15-17] or chlorine in the $TiCl_4/H_2O$ process,[18,19] the latter being difficult to remove at low temperatures.[20] However, the choice of metal precursor is important, as the lowest deposition temperatures have been employed using alkyl-based precursors, resulting in very low impurity concentrations in the films. This is especially evident in Al_2O_3,[4,15,16,21-23] PtO_x,[24,25] and ZnO,[7,8] as the alkyl ligands are highly reactive and labile. It is also the oxidants that play an important role, particularly in terms of reactivity. Films of fair to good quality are possible at lower temperatures where more reactive precursors, such as ozone or an oxygen plasma, are employed. The high reactivity of the plasma is attributed to the fact that it contains reactive ionic and radical oxygen species, which makes it an appealing candidate for obtaining high purity films at temperatures as low as room temperature.[26] For this reason, we have been investigating the potential of plasma-enhanced ALD as a route to Al_2O_3, TiO_2, and Ta_2O_5 thin films at temperatures down to 25°C. This paper describes the work carried out, using a variety of metal precursors, and compare the results with thermal ALD processes from the literature.

Experimental

The experiments were carried out on three remote plasma ALD reactors. The home-built ALD-I reactor and the commercially built Oxford Instruments FlexAL reactor are described in detail elsewhere.[22] The Oxford Instruments OpAL apparatus, an open-load system, was employed for the deposition of Al_2O_3 and operates in a similar manner to the FlexAL, although without a turbo pump. The base pressure was ~1 mTorr for the OpAL and ~10^{-3} mTorr for the ALD-I and FlexAL, and typical operating pressures were 100–

* Electrochemical Society Active Member.
z E-mail: s.e.potts@tue.nl; w.m.m.kessels@tue.nl

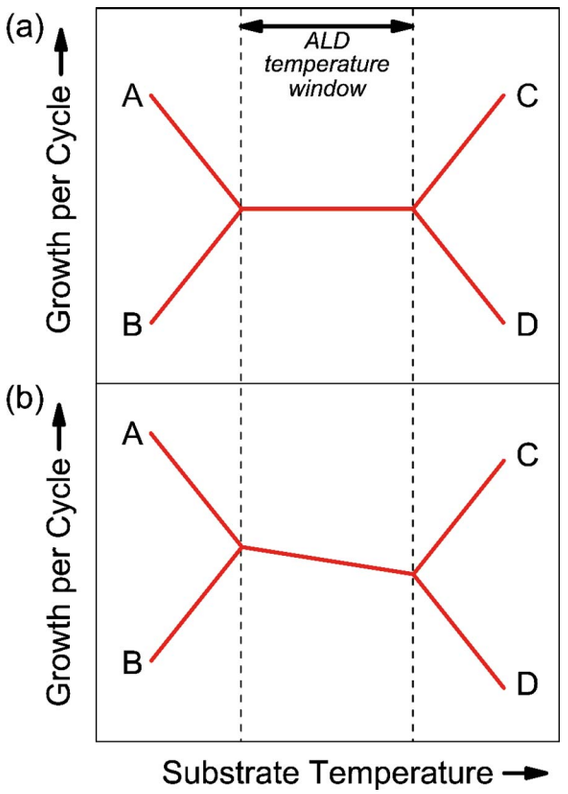

Figure 1. (Color online) A schematic representation of (a) an ideal ALD temperature window, where it is assumed that a sub-monolayer has been deposited per cycle and (b) a more commonly observed ALD window (especially for metal oxides), showing a slight reduction in growth per cycle with increasing temperature.

1000 mTorr (OpAL) and 7.5–100 mTorr (ALD-I and FlexAL). Al_2O_3 was deposited using OpAL and FlexAL, TiO_2 using FlexAL and ALD-I, and Ta_2O_5 using FlexAL. The Ta_2O_5 results on FlexAL are compared with our previous work using ALD-I.[27] The compounds $[Al(CH_3)_3]$ (Sigma Aldrich), $[Ti(O^iPr)_4]$ (Sigma Aldrich), novel Cp-based ALD precursors $[Ti(Cp^{Me})(O^iPr)_3]$ (donated by SAFC Hitech, Ltd.) and $[TiCp^*(OMe)_3]$ (donated by Air Liquide), and $[Ta(NMe_2)_5]$ (STREM Chemicals Ltd.), all having a purity of >99.9%, were employed as precursors[a] and were contained in stainless steel bubblers. Oxygen (purity >99.999%) was used to form the plasma, and argon (purity >99.999%) was employed as the purge gas. For the processes employing $[Al(CH_3)_3]$, $[Ti(Cp^{Me})(O\ ^iPr)_3]$, and $[TiCp^*(OMe)_3]$, the oxygen flow was continuous throughout the entire process, but where $[Ti(O^iPr)_4]$ and $[Ta(NMe_2)_5]$ were used, the flow was restricted to the plasma step. Water (VWR, GBR Rectapur grade, >99.999%) used in thermal ALD experiments was also held in a stainless steel bubbler at either ambient temperature (FlexAL) or 19°C (OpAL) to reduce the vapor pressure and prevent overdosing. The substrates were n-type Si(100) wafers, which were 100 mm in diameter for the FlexAL and OpAL reactors and ~40 × 40 mm for ALD-I. These wafers were covered with a thin native oxide (SiO_2) layer and did not undergo any additional cleaning steps. The ALD conditions for each process are summarized in Table II. Film growth during the ALD process was monitored by in situ spectroscopic ellipsometry (SE), carried out using a J. A. Woollam Inc. M2000 rotating compensator ellipsometer.[27,28] The atomic composition of the films was determined by Rutherford backscattering spectroscopy (RBS), except for the hydrogen concentration, which was obtained by elastic recoil detection (ERD) analysis. The detection limits for the RBS and ERD measurements are not the same for each set of measurements and were quoted where appropriate. The mass density of the films was calculated using a combination of the RBS and SE data.

Table I. Examples of low temperature ALD of metal oxides deposited below 150°C.

Material	Metal precursor	Oxidant	Lowest reported temperature (°C)	Reference
Al_2O_3	$[Al(CH_3)_3]$	H_2O	33	6
Al_2O_3	$[Al(CH_3)_3]$	O_3	25	30
Al_2O_3	$[Al(CH_3)_3]$	O_2 plasma	25	4, 15, 16, and 21-23
TiO_2	$TiCl_4$	H_2O	100	18 and 19
TiO_2	$TiCl_4$	H_2O_2	100	34
TiO_2	$[Ti(O\ ^iPr)_4]$	H_2O	150	35 and 36
TiO_2	$[Ti(O\ ^iPr)_4]$	H_2O_2	77	37
Ta_2O_5	$TaCl_5$	H_2O	80	42
Ta_2O_5	$[Ta(NMe_2)_5]$	H_2O	150	45 and 46
Ta_2O_5	$[Ta(NMe_2)_5]$	O_2 plasma	100	27
PtO_x	$[Pt(acac)_2]$	O_3	120	24
PtO_2	$[Pt(Cp^{Me})Me_3]$	O_2 plasma	100	25
ZnO	$[Zn(CH_2CH_3)_2]$	H_2O	60	7
ZnO	$[Zn(CH_2CH_3)_2]$	H_2O_2	25	8

Results and Discussion

The plasma-enhanced ALD of Al_2O_3, TiO_2, and Ta_2O_5 has been investigated at substrate temperatures down to 25°C. Every process was routinely monitored using in situ SE to determine the film thickness. The slope of the resulting thickness vs ALD cycles plot gave the growth per cycle for the process (an example for the depositions at 100°C is shown in Fig. 2). All ALD processes showed linear growth at every deposition temperature reported in this paper (with the exception of the TiO_2 depositions from $[Ti(O^iPr)_4]$ at substrate temperatures >250°C), with no significant nucleation delay.

Aluminum oxide.— Al_2O_3 has been a material of high interest with respect to ALD (see the review by Puurunen).[3] However, it is relatively recently that low substrate temperatures have been investigated. The growths per cycle of two of the most-reported thermal processes are compared with the plasma-enhanced route in Fig. 3. We deposited Al_2O_3 using both the plasma-enhanced and thermal processes on an Oxford Instruments FlexAL reactor[21] and OpAL reactor. The growth of the plasma-enhanced method showed a gradual decrease from 0.17 nm/cycle at 25°C to 0.11 nm/cycle at 300°C. The decrease was essentially linear, with the exception of the runs at 25 and 50°C, which were slightly higher. The corresponding thermal process showed a maximum value of 0.10 nm/cycle at 200–250°C. Our results for the thermal process differ from those of Groner et al.,[6] where the growth was higher at ~0.13 nm/cycle. These two thermal processes were carried out in different reactors and were clearly optimized at different temperatures (where the peak of the data is). A possible reason for such a difference in growth per cycle is the water dose. Increasing the water dose (i.e., the mass of water per unit time) leads to an increase in growth per cycle without affecting the film composition,[29] as more surface hydroxyl groups are created with higher doses. So despite the difference in water dose time (20 ms for our work, 2 s for Groner et al.), it is likely that our water flow rate was lower, affording a lower growth per cycle, because the water on the OpAL reactor was actively cooled to 19°C to avoid overdosing. The reduction

[a] acac is acetylacetonate, $CH(C{=}OCH_3)_2$; Cp^{Me} is monomethylcyclopentadienyl, η^5-$C_5H_4(CH_3)$; Cp^* is pentamethylcyclopentadienyl, η^5-$C_5(CH_3)_5$; Me is methyl, CH_3; and ^iPr is isopropyl, $CH(CH_3)_2$.

Table II. The ALD process conditions for the metal oxides reported in this work. The purges for the ALD processes where $[Ti(Cp^{Me})(O^iPr)_3]$ and $[TiCp^*(OMe)_3]$ were used only incorporated an argon flow for part of the duration. In these cases, the pumping and argon (Ar) times are given in the order they occurred during the purge. In all other cases, a continuous Ar flow was employed throughout the cycle. "Oxidant" refers to an O_2 plasma for plasma-enhanced ALD and water for thermal ALD. The conditions for the Ta_2O_5 process on the ALD-I reactor are reported elsewhere.[27]

Variable	Al_2O_3	Al_2O_3	TiO_2	TiO_2	TiO_2	Ta_2O_5
ALD	Plasma-enhanced	Thermal	Plasma-enhanced	Plasma-enhanced	Plasma-enhanced	Plasma-enhanced
Reactor	OpAL and FlexAL	OpAL and FlexAL	FlexAL	ALD-I	ALD-I	FlexAL
Precursor	$[Al(CH_3)_3]$	$[Al(CH_3)_3]$	$[Ti(O^iPr)_4]$	$[Ti(Cp^{Me})(O^iPr)_3]$	$[TiCp^*(OMe)_3]$	$[Ta(NMe_2)_5]$
$T_{substrate}$	25–400°C	25–400°C	25–400°C	100–400°C	50–300°C	25–250°C
$T_{precursor}$	~25°C	~25°C	45°C	70°C	110°C	65°C
Precursor dose	0.02 s	0.05 s	4 s	5 s	4 s	5 s
Precursor purge	3 s	10 s	4 s	4 s pumping, 4 s Ar	4 s pumping, 2 s Ar, 2 s pumping	5 s
Plasma power	400 W	—	400 W	100 W	100 W	200 W
Oxidant time	2 s	0.02 s	12 s	5 s	5 s	5 s
Oxidant purge	0.5 s	10 s	1.5 s	2 s pumping, 0.5 s Ar, 2 s pumping	4 s pumping	15 s
O_2 flow	60 sccm	—	60 sccm	7.5 mTorr	7.5 mTorr	50 sccm
Ar flow	20 sccm	200 sccm	30 sccm	15 mTorr	15 mTorr	100 sccm (precursor step), 150 sccm (purges), 50 sccm (plasma)

in growth per cycle for the thermal ALD process with decreasing temperature below the maximum value appears to be a result of insufficient thermal energy for the reaction between water and the methyl surface groups to occur as rapidly, resulting in fewer reactive hydroxyl surface groups with which $[Al(CH_3)_3]$ can react. Unlike water, the oxygen plasma is sufficiently reactive with the surface methyl groups down to room temperature, resulting in an almost linear decrease in growth per cycle from 25–300°C. At higher deposition temperatures for the thermal processes with water, the growth per cycle profile follows that of the plasma-enhanced process. The decrease in growth per cycle, as illustrated in Fig. 1b, is due to the gradual reduction of reactive surface groups, such as hydroxyls, with increasing deposition temperature.[5,12,15,16]

Another important consideration is the oxidant purge time (Fig. 4). The post-plasma purge times required (0.5 s) were significantly lower than those required to purge water from the system in the thermal process (10 s for this work and 5–180 s for Groner et al.[6]), which allows for a significantly reduced overall cycle time for the plasma-enhanced process. The thermal ALD process employing ozone as the oxidant reported by Kim et al.[30] gave the lowest growth per cycle above 100°C (~0.09 nm/cycle). Ozone is more reactive than water toward the surface methyl groups, forming hydroxyl, methoxy, formate, and carbonate surface groups in the process.[31,32] Therefore, Kim et al. suggested that the dramatic increase in growth per cycle observed at deposition temperatures below 100°C was attributed to the insufficient removal of the aforementioned oxygen-based surface groups in the steps subsequent to the oxidation because there was insufficient thermal energy with which to remove them.[30] Also in this case, the ozone purge was kept constant at 3 s at 33–100°C, where a longer purge at lower temperatures may have helped to reduce the impurities. In comparison, our plasma-

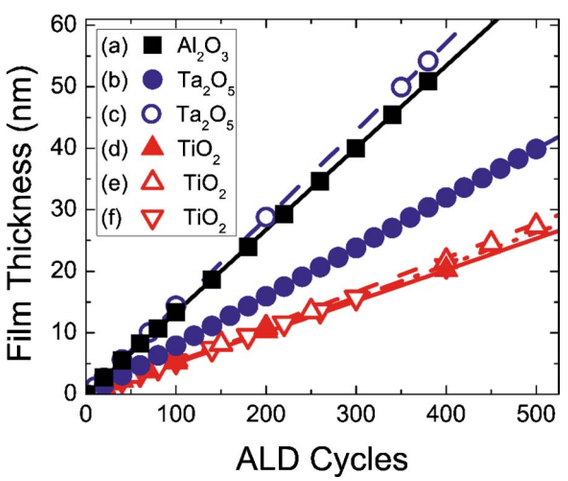

Figure 2. (Color online) The increase in film thickness with the number of ALD cycles as measured by in situ SE (deposition temperature = 100°C). The increase was linear for each precursor: (a) $[Al(CH_3)_3]$, (b) $[Ta(NMe_2)_5]$ (ALD-I reactor),[27] (c) $[Ta(NMe_2)_5]$ (FlexAL reactor), (d) $[Ti(O^iPr)_4]$, (e) $[Ti(Cp^{Me})(O^iPr)_3]$, and (f) $[TiCp^*(OMe)_3]$.

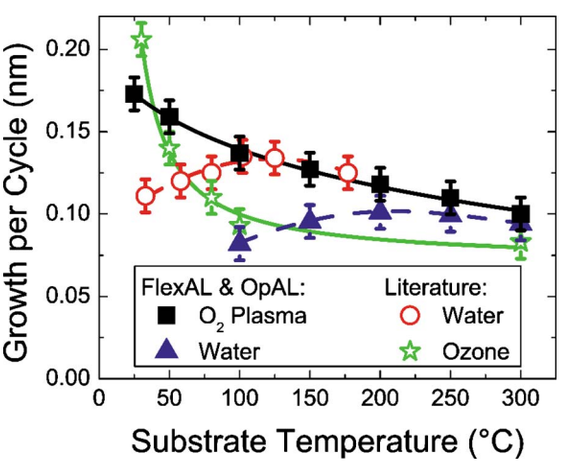

Figure 3. (Color online) A comparison of growths per cycle for the ALD of Al_2O_3 from $[Al(CH_3)_3]$. Shown here are the thermal process with water, as reported by Groner et al.,[6] the thermal process with ozone, as reported by Kim et al.,[30] and our plasma-enhanced (FlexAL) and thermal processes (FlexAL and OpAL combined).[21] All lines serve as a guide to the eye.

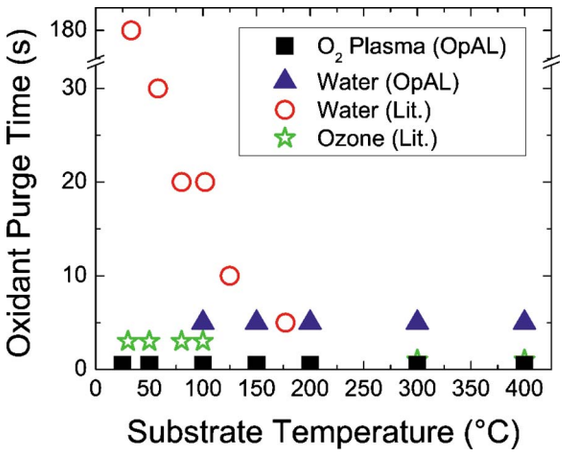

Figure 4. (Color online) A comparison of the oxidant purges required for various Al_2O_3 ALD processes: the plasma-enhanced and thermal processes on OpAL, the thermal process with water (note the break in the scale), as reported by Groner et al.,[6] and the thermal process with ozone, as reported by Kim et al.[30,48]

enhanced route gave a more consistent growth per cycle profile down to 25°C and provided the highest growths per cycle over 50–300°C with the shortest cycle times.

In terms of film composition, the films deposited by both thermal and plasma-enhanced ALD in this work were over-stoichiometric at deposition temperatures below 200°C (Fig. 5a). The similar reduction in hydrogen content (Fig. 5b) with increasing substrate temperature suggests that this is due to the incorporation of hydroxyl groups in the film.[16] In all cases, the carbon content was below the RBS detection limit (1 atom %); although thermal effusion measurements have suggested that a small quantity of carbon was present in the films deposited by this process.[17] The mass density (Fig. 5c) was ~3.0 g cm^{-3} at deposition temperatures of 200°C and above for the plasma-enhanced process, which is close to the bulk value of Al_2O_3 (3.1 g cm^{-3}).[33] A gradual decrease was observed below 200°C to a minimum of 2.6 g cm^{-3} at 25°C. This decrease in mass density is likely to be the result of excess –OH in the film, which accounts for the higher than expected growths per cycle obtained below 100°C. The thermal water process showed no significant difference in terms of impurity content, and the mass density of the films over the temperature range was still within error, although slightly lower than that for the plasma-enhanced process. The thermal process with ozone gave over-stoichiometric films at all temperatures up to 300°C with up to 5 atom % carbon contamination.[30]

The growth per cycle profiles are apparently all different, which, in part is caused by the varying mass densities. However, determination of the number of (metal) atoms deposited per cycle, obtained by dividing the atom density from RBS by the total number of ALD cycles, can show if this is the case. For example, if the number of atoms deposited per cycle does not vary significantly over a temperature range, any variation in growth per cycle is most likely due to the variation in mass density; however, if there is a difference in atoms deposited, other factors, such as chemical vapor deposition (CVD) or surface group loss, may be occurring. Figure 6 shows the growth per cycle data for the plasma-enhanced and thermal processes on both the FlexAL and OpAL reactors and the number of Al atoms deposited per cm^2 in a cycle. In terms of films deposited by plasma-enhanced ALD, there is no significant difference between the growths per cycle from either reactor; but for the thermal process, more atoms appear to have been deposited by the OpAL reactor. The OpAL reactor is not equipped with a turbo pump or load lock, so it may not be able to purge the water away as effectively as in the FlexAL reactor and the chamber vacuum has to be disrupted for sample loading. However, a greater difference in mass density

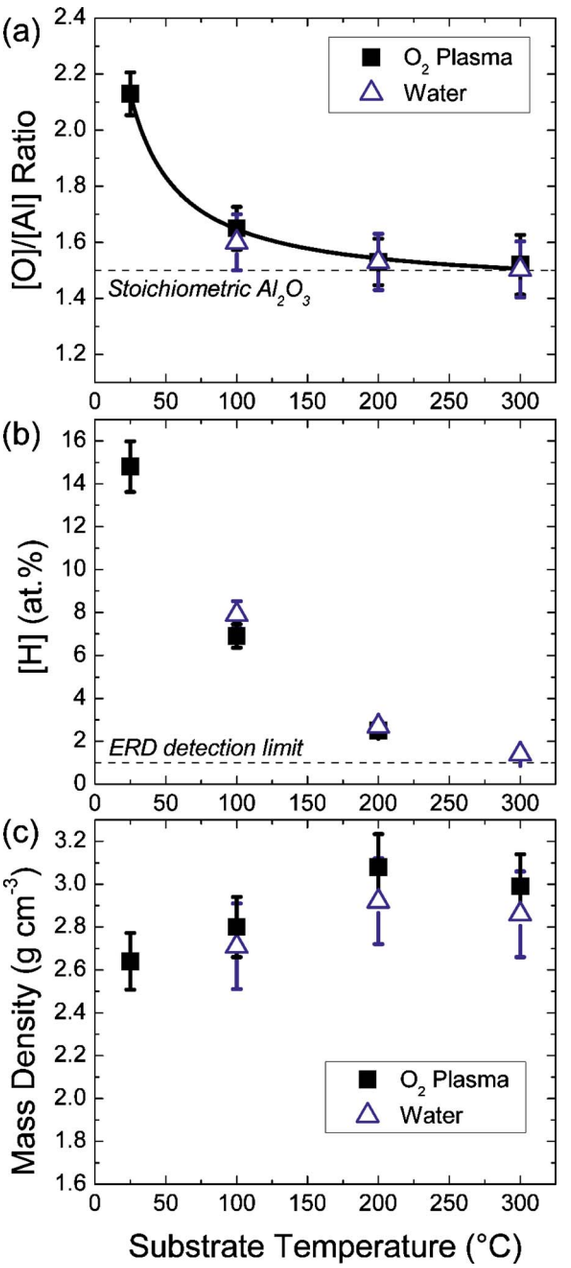

Figure 5. (Color online) The film characteristics of the Al_2O_3 films obtained on the OpAL reactor. (a) The [O]/[Al] ratio of the films (the line serves as a guide to the eye), (b) the hydrogen content of the films, and (c) the mass density of the films.

would be expected for such a difference in Al atoms deposited per cycle where the growth per cycle remains the same. There is a clear gradient for Al atoms deposited per cycle with the plasma-enhanced process, showing the effect of dehydroxylation (loss of surface groups) with increasing substrate temperature. A similar gradient was observed for the growth per cycle, although this is enhanced at 25 and 50°C as a result of the decreased film density and increased OH concentration (as shown in Fig. 5). For the thermal processes, the effect of lower temperatures is clear; with the number of Al atoms deposited being half of that of the plasma-enhanced process at 100°C, suggesting that the rate of reaction is lower at these temperatures. The temperature at which the thermal process was optimized (i.e., the saturation of each ALD step was determined, which was

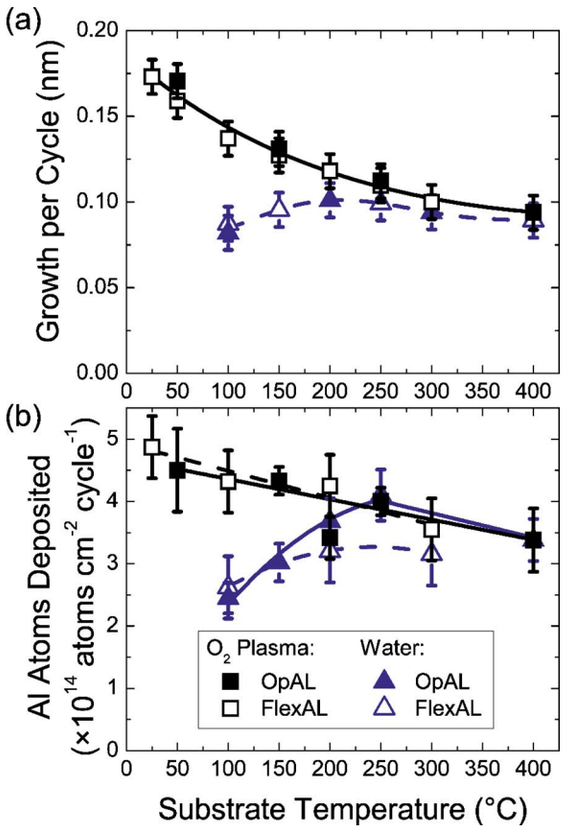

Figure 6. (Color online) (a) The growths per cycle for plasma-enhanced and thermal ALD of Al_2O_3 on both the OpAL and FlexAL reactors. (b) The Al atoms deposited per cm^2 in a cycle. All lines serve as a guide to the eye.

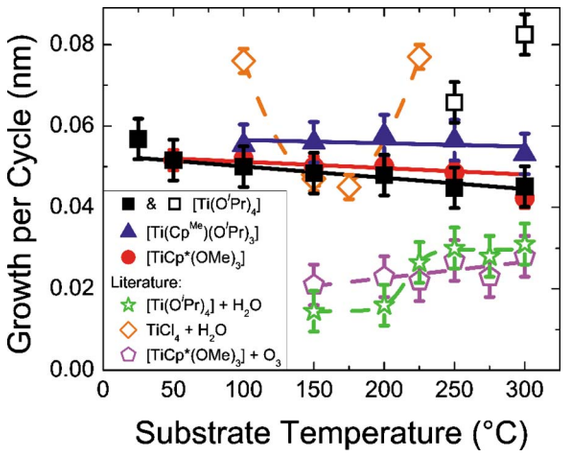

Figure 7. (Color online) A comparison of growths per cycle for the ALD of TiO_2. Shown here are thermal processes: $TiCl_4$ and water, as reported by Aarik et al.[18,19] $[Ti(O^iPr)_4]$ and water, as reported by Ritala et al.[35,36] and $[TiCp^*(OMe)_3]$ and ozone, as reported by Katamreddy et al.[40] These are compared to the plasma-enhanced processes using $[Ti(O^iPr)_4]$, $[Ti(Cp^{Me})(O^iPr)_3]$ and $[TiCp^*(OMe)_3]$.[38] The higher growths per cycle for $[Ti(O^iPr)_4]$ resulting from anatase formation are shown as hollow squares. Lines serve as a guide to the eye.

200°C in these cases) apparently gave the highest growth per cycle and the highest number of Al atoms deposited. At higher temperatures, the growth per cycle and atoms per cycle decrease in line with the plasma-enhanced process as a result of the loss of surface groups.

In summary, the plasma-enhanced ALD of Al_2O_3 generally gives a higher growth per cycle at low temperatures than the corresponding thermal processes using water or ozone, although the temperature at which the thermal process is optimized and the water flow rate play an important role. The film compositions of the plasma-enhanced and thermal processes were comparable, with the concentration of –OH increasing with decreasing substrate temperature. Carbon was not detected in the films (RBS detection limit = 1 atom %). Analysis of the Al atoms deposited per cycle showed that the temperature window could easily be extended down to room temperature with fixed cycle settings for the plasma-enhanced ALD of Al_2O_3. For the thermal process, temperatures lower than the optimization temperature could be considered outside the temperature window; however, if saturation curves were determined for each deposition temperature and the water flow rate were increased, this could be overcome.

Titanium dioxide.— TiO_2 is a well-studied ALD material,[18,19,34-37] and a selection of the low temperature ALD studies is summarized in Fig. 7. For the plasma-enhanced ALD of TiO_2, we employed $[Ti(O^iPr)_4]$, $[Ti(Cp^{Me})(O^iPr)_3]$, and $[TiCp^*(OMe)_3]$ as precursors.[38] The heteroleptic mono Cp-based alkoxides are not sufficiently reactive with water during ALD,[39] but they are reactive with ozone[40] and an oxygen plasma. The growths per cycle for our plasma-enhanced processes were 0.05–0.06 nm/cycle, over the deposition temperature range 100–250°C. The growths per cycle using $[Ti(Cp^{Me})(O^iPr)_3]$ were slightly higher than those of the other two Ti precursors, as more Ti atoms were deposited per cycle for this precursor (Fig. 8a). Again, a gradual decrease in growth per cycle was observed with increasing substrate temperature for all of the Ti precursors, which can be attributed to increasing mass density. The loss of surface groups is not likely to be a significant factor for the Cp-based precursors, as the Ti atoms deposited per cycle were constant over the temperature range. At 25°C, the growth per cycle obtained using $[Ti(O^iPr)_4]$ was higher than the expected trend, which is a result of the excess OH groups in the film, as for the Al_2O_3 films (Fig. 8b-d). All precursors gave significantly higher growths per cycle with the plasma-enhanced ALD process than for those obtained for the thermal routes using $[Ti(O^iPr)_4]$ and water, as reported by Ritala et al.[35] and Rahtu and Ritala,[36] and $[TiCp^*(OMe)_3]$ and ozone, as reported by Katamreddy et al.[40] This shows the benefits of the high reactivity of the plasma; although it is somewhat surprising that ozone, itself a highly reactive gas, could not allow for a higher growth per cycle. The growths per cycle of the $TiCl_4$ and water process were extended down to 100°C by Aarik et al.[18,19] The data were more comparable to the plasma-enhanced process at substrate temperatures around 150°C because $TiCl_4$ is more reactive toward surface groups than $[Ti(O^iPr)_4]$ (see Fig. 7). The lower data points for the $TiCl_4$/water process at 150 and 175°C were reported to be the result of etching of the film by HCl formed during the ALD process at these temperatures.[19] The increase in growth per cycle at higher temperatures for the $TiCl_4/H_2O$ process was attributed to the crystallization of the films, and below 150°C the increase was due to the condensation of water on the substrate, leading to a dramatic increase in surface hydroxyl groups. The presence of such additional surface groups at low temperatures was less prominent for the plasma-enhanced ALD using $[Ti(O^iPr)_4]$, $[Ti(Cp^{Me})(O^iPr)_3]$, and $[TiCp^*(OMe)_3]$.

The number of Ti atoms deposited per cycle is shown in Fig. 8a. For the two Cp-based precursors, the Ti deposited was generally consistent across the temperature ranges studied, implying that these precursors are less affected by surface dehydroxylation than $[Al(CH_3)_3]$ in the Al_2O_3 process, where there is a distinct negative gradient in the data (Fig. 5b). The data also complement the growth per cycle values in Fig. 7, whereby $[Ti(Cp^{Me})(O^iPr)_3]$ deposited

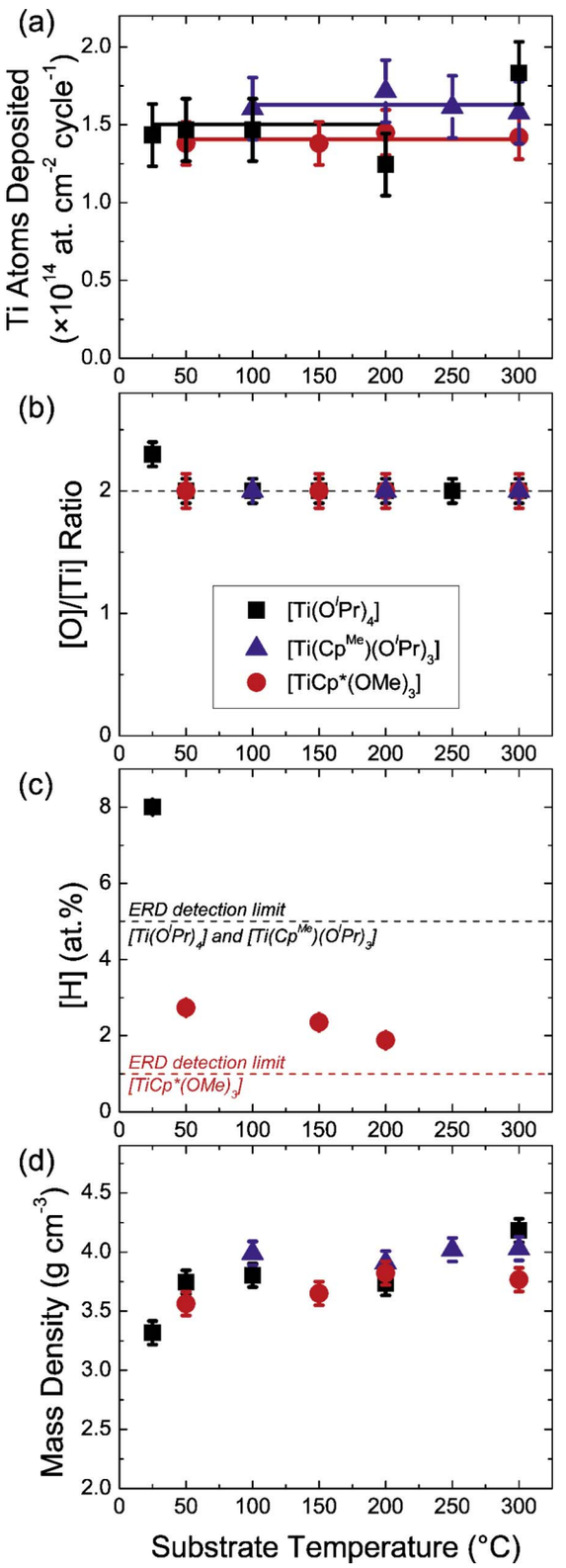

Figure 8. (Color online) Compositional details of the TiO_2 films deposited by plasma-enhanced ALD. (a) The Ti atoms deposited per cycle, (b) the [O]/[Ti] ratio (the ratio for stoichiometric TiO_2 being represented by a dashed line), (c) the hydrogen content, and (d) the mass density of the films.

more Ti atoms per cycle and afforded a higher growth per cycle, when compared with $[TiCp^*(OMe)_3]$. In addition to the experimental inaccuracy of RBS, the $[Ti(O^iPr)_4]$ is not so straightforward, as there is no real, clear-cut linear trend. The rise in Ti atoms deposited at 300°C can be attributed to the decomposition (CVD) of the precursor, as a significant amount of carbon (~17 atom %) was present in films deposited at that temperature. For depositions using $[Ti(O^iPr)_4]$ at temperatures ≥250°C, crystallization was observed in the anatase form, resulting in higher growths per cycle.[28] At 250 and 300°C, the growth began in the amorphous phase at a lower growth per cycle, after which anatase TiO_2 was deposited at a much higher rate. The transitions were observed between 400–700 cycles at 250°C and above 200 cycles at 300°C. Where $[Ti(Cp^{Me})(O\ ^iPr)_3]$ was the precursor, anatase TiO_2 was also observed at substrate temperatures ≥250°C, but this did not seem to have such a dramatic effect on the growth per cycle, suggesting that the Cp^{Me} group inhibits the anatase formation to some extent.

In terms of film composition, films deposited by plasma-enhanced ALD from all of our Ti precursors gave stoichiometric TiO_2 at 50°C and above (Fig. 8b). The film from $[Ti(O^iPr)_4]$ at 25°C was over-stoichiometric, which, as with the $[Al(CH_3)_3]$/water process, is the result of the incorporation of hydroxyl groups in the film, evident by the 8 atom % hydrogen present (Fig. 8c) and the lower mass density of the film (Fig. 8d). At other temperatures, the carbon and hydrogen concentrations were below their detection limits for RBS and ERD (1 and 5 atom %, respectively) where $[Ti(O^iPr)_4]$ was the precursor. The stoichiometry of the films deposited by $[Ti(Cp^{Me})(O^iPr)_3]$ and $[TiCp^*(OMe)_3]$ were the same as those obtained using $[Ti(O^iPr)_4]$ (and so the data overlap in Fig. 8b), and no carbon was detected at any temperature for the Cp-based precursors. Hydrogen was detected in the films from $[TiCp^*(OMe)_3]$ (2–3 atom %), and similar quantities are possibly present in the films from the other two precursors, as the detection limit in those experiments was higher. As such, it is difficult to directly compare the hydrogen content of our films with those of Ritala et al.,[35] as they reported a hydrogen content of ~0.3 atom % (measured using nuclear reaction analysis with a $^{15}N^{2+}$ beam), which is below the lowest detection limit (1 atom %) for ERD in our experiments. The films grown from $TiCl_4$ and water at 100°C were also stoichiometric but contained 1.2 atom % chlorine, which can lead to films with a high surface roughness, due to the aforementioned etching.[41] In terms of mass density (Fig. 8d), the films deposited by all precursors had densities over the range 3.6–4.2 g cm^{-3}, which is comparable to the bulk density of anatase TiO_2 (3.9 g cm^{-3}).[33] The films from $[Ti(O^iPr)_4]$ had the most variation in density owing to the larger experimental inaccuracy in the RBS experiments. The low density at 25°C was a result of –OH incorporation as mentioned previously, whereas the higher density of 4.18 g cm^{-3} at 300°C is likely to be a result of the crystallization. For the noncrystalline films below 200°C, the high density is a feature of the plasma-enhanced ALD method.

The plasma-enhanced ALD processes TiO_2 using $[Ti(O^iPr)_4]$, $[Ti(Cp^{Me})(O^iPr)_3]$, and $[TiCp^*(OMe)_3]$ afford higher growths per cycle compared with the $[Ti(O^iPr)_4]$ and water process. They were preferable to the $TiCl_4/H_2O$ process, in that the possibility of the films containing chlorine is negligible. The films grown in this study were consistently stoichiometric down to 50°C.

Tantalum oxide.— Ta_2O_5 is another thoroughly studied ALD material, particularly via thermal routes using halide-,[42,43] alkoxide-,[44] and amide-based[27,45,46] precursors. However, films grown at <150°C are not so commonly known. We recently reported the low temperature plasma-enhanced ALD of Ta_2O_5 using $[Ta(NMe_2)_5]$ on the ALD-I reactor,[27] which gave a growth of ~0.08 nm/cycle over the temperature range 100–225°C (Fig. 9), which is comparable to the $TaCl_5$/water process above 100°C.[42] All films were stoichiometric Ta_2O_5 with a [O]/[Ta] ratio of 2.5 and

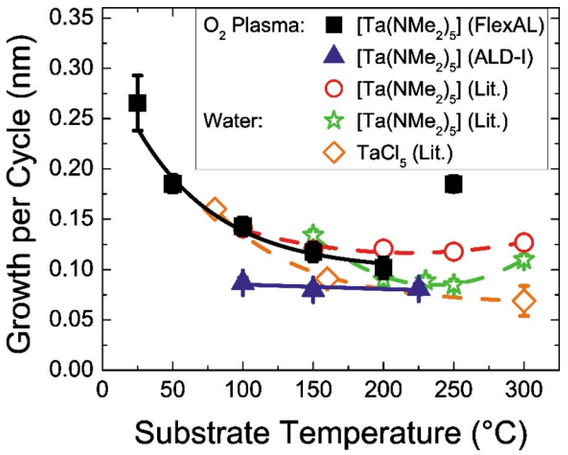

Figure 9. (Color online) A comparison of growths per cycle for the ALD of Ta_2O_5 from $[Ta(NMe_2)_5]$. Shown here are the thermal process with water and the plasma-enhanced process, as reported by Maeng et al.[45,46] and our plasma-enhanced processes on ALD-I[27] and FlexAL. The $TaCl_5/H_2O$ process is also shown for comparison.[42] Lines serve as a guide to the eye.

contained hydrogen (Fig. 10c). No nitrogen or carbon was detected. The mass density varied from 7.8 g cm^{-3} at 100°C to 8.1 g cm^{-3} at 225°C, which is comparable to the bulk density value of Ta_2O_5 (8.24 g cm^{-3}).[33] Maeng et al. previously carried out a comparison of the thermal and plasma-enhanced ALD of Ta_2O_5 from $[Ta(NMe_2)_5]$ using water and an oxygen plasma, respectively.[45,46] The thermal process afforded comparable growths, ~0.085 nm/cycle, to those obtained in our plasma-enhanced process at 200–300°C (Fig. 9). The growths per cycle for the thermal process increased at both the higher and lower substrate temperatures due to precursor decomposition (CVD) and condensation of water, respectively. The plasma-enhanced ALD of Ta_2O_5 using $[Ta(NMe_2)_5]$ reported by Maeng and co-workers gave much higher growths per cycle of ~0.12 nm. These films had a [O]/[Ta] ratio of 2.6, and no nitrogen or carbon incorporation was reported (the hydrogen content was not commented upon). The mass density reported, ~7.75 g cm^{-3} (94% of the bulk value of Ta_2O_5 although the precise substrate temperatures were not reported), was slightly lower than our previously reported values,[27] but this difference cannot be the reason for such a significant difference in growth. It may be a result of the use of different ALD equipment, where the design of the reactor may affect the way in which precursors are introduced to the substrate. With the exception of our results, plasma-enhanced ALD using $[Ta(NMe_2)_5]$ afforded higher growths per cycle than the $TaCl_5$/water process, although the $[Ta(NMe_2)_5]$/water process gave similar growths per cycle.

To investigate the use of different reactors, the $[Ta(NMe_2)_5]$ plasma-enhanced ALD process was transferred to from the ALD-I to the FlexAL reactor, extending the investigation down to 25°C. The growths per cycle obtained bore more resemblance to the results of Maeng et al. than those obtained using ALD-I. The increase in growth per cycle at temperatures below 100°C was significant, which was again a result of the low mass density of the film as the number of Ta atoms deposited did not change dramatically over the temperature range (Fig. 10a and d). At 250°C, there was also an increase in growth per cycle, due to the decomposition of the $[Ta(NMe_2)_5]$ precursor. This was consistent with the thermogravimetric analysis of the precursor in the literature,[47] which showed the onset of decomposition at around 200°C. The effect of the CVD is clearly shown by the almost twofold increase in the Ta deposited at 250°C, and to a much lesser extent at 200°C.

Despite the similarity in the numbers of atoms being deposited per cycle between the ALD-I and FlexAL reactors, the film compo-

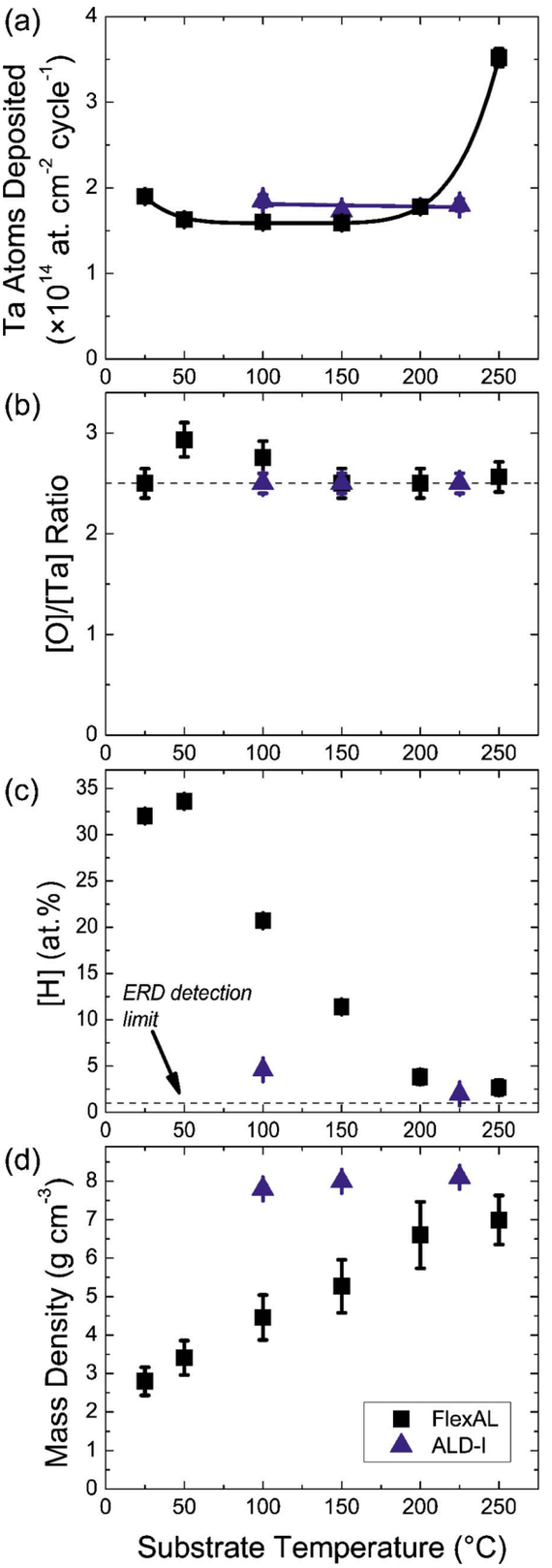

Figure 10. (Color online) Compositional data for the Ta_2O_5 films deposited on the FlexAL and ALD-I reactors. (a) Ta atoms deposited per cycle (lines serve as a guide to the eye), (b) [O]/[Ta] ratio, the ratio of stoichiometric Ta_2O_5 is represented by a dashed line, (c) the hydrogen concentration, and (d) the mass densities of the films.

sitions were different (Fig. 10b-d). The films deposited on the ALD-I reactor had a density close to that of the bulk, were stoichiometric Ta_2O_5, and contained very low concentrations of hydrogen. At 50 and 100°C on the FlexAL reactor, the films were overstoichiometric with an excess of oxygen (Fig. 10b). The films also contained signifiant concentrations of hydrogen (up to 35 atom %), which are very high when compared with the Al_2O_3, TiO_2, and other Ta_2O_5 processes. However, in common with these processes, the hydrogen concentration decreased with increasing substrate temperature. It is likely that there is a significant presence of OH groups in the film; therefore, it might just be coincidence that the film at 25°C was stoichiometric, as there was a significant presence of hydrogen and oxygen in that film. Carbon and nitrogen were not detected at any temperature (RBS detection limit = 5 atom % in each case). There was a positive correlation between substrate temperature and film density (Fig. 10d), but the densities were much lower than expected for a good ALD film, less than half the bulk value below 50°C. This does not compare with the 94% of the bulk value reported by Maeng et al.,[46] despite similar growths per cycle, probably due to the excess of hydroxyl groups. Why the film densities were low and hydroxyl groups were present in such high quantities and why the mass densities were so low, is still unclear. The differences observed between the two reactors could be a result of the composition of the plasmas used, which interact with the NMe_2 ligands in different ways. However, such a difference in growth per cycle and film density has not been observed for other processes. A possible reason is that the ion flux and ion energies in the ALD-I system are generally higher than in the FlexAL reactor. The plasma composition in all reactors and the effects on film growth are currently under investigation.

Conclusions

We have deposited Al_2O_3, TiO_2, and Ta_2O_5 thin films using plasma-enhanced ALD and addressed the ability of plasma-enhanced ALD to deposit metal oxide thin films at temperatures as low as room temperature. Analysis of the metal atoms deposited per cycle provided a clearer view as to where the edges of the temperature window were and complemented the generally accepted growth per cycle version. With this in mind, the temperature windows for the Al_2O_3, TiO_2, and Ta_2O_5 processes have been extended down to 25, 50, and 100°C, respectively.

For Al_2O_3, the film compositions were comparable to those deposited by the related thermal ALD processes down to 150°C. The film quality was fair to good down to room temperature. The carbon and hydrogen contents of the Al_2O_3 films did not differ significantly from those of the thermal process, but the cycle time was reduced significantly because of the relatively short plasma purge of 0.5 s. Also, the Al_2O_3 growths per cycle were higher than the corresponding thermal processes with water without compromising the film quality. The plasma was also sufficiently reactive to remove carbon-containing surface groups at temperatures below 100°C, which ozone did not. In TiO_2, $[Ti(O^iPr)_4]$, $[Ti(Cp^{Me})(O^iPr)_3]$, and $[TiCp^*(OMe)_3]$ precursors gave higher growths per cycle than the thermal $[Ti(O^iPr)_4]$/water and $[Ti(Cp^{Me})(O^iPr)_3]$/ozone, demonstrating the advantage, in this case, of the increased reactivity of the plasma. In fact, the use of a plasma or ozone is a necessity with the Cp-based precursors, as they are sparingly reactive with water during ALD. For Ta_2O_5 from $[Ta(NMe_2)_5]$, the films were stoichiometric down to 150°C on the FlexAL reactor and the growths per cycle observed were comparable to those reported for the plasma-enhanced route. On the ALD-I reactor, the growths per cycle were lower but the films were stoichiometric down to 100°C and contained less hydrogen. The film densities varied considerably, depending on the reactor.

In summary, the use of an oxygen plasma has the benefits of reducing the cycle time and giving higher growths per cycle than corresponding thermal processes due to its high reactivity. Analysis of atoms deposited per cycle aids in the clarification of where the boundaries of the temperature window lie as it is not affected by variations in film density.

Acknowledgments

The research leading to these results has received funding from the European Community's Seventh Framework Programme (FP7/2007-2013) under grant agreement number CP-FP213996-1. The authors thank L. R. J. G. van den Elzen, J. C. Goverde, and D. Hoogeland for their assistance in the depositions and J. J. A. Zeebregts, M. J. F. van de Sande, and C. A. A. van Helvoirt for their technical assistance, support, and advice. SAFC Hitech Ltd. and Air Liquide are also thanked for their donations of $[Ti(Cp^{Me})(O^iPr)_3]$ and $[TiCp^*(OMe)_3]$, respectively.

Eindhoven University of Technology assisted in meeting the publication costs of this article.

References

1. T. Suntola, *Mater. Sci. Rep.*, **4**, 261 (1989).
2. J. Niinistö, M. Ritala, and M. Leskelä, *Mater. Sci. Eng., B*, **41**, 23 (1996).
3. R. L. Puurunen, *J. Appl. Phys.*, **97**, 121301 (2005).
4. E. Langereis, M. Creatore, S. B. S. Heil, M. C. M. van de Sanden, and W. M. M. Kessels, *Appl. Phys. Lett.*, **89**, 081915 (2006).
5. C.-Y. Chang, F.-Y. Tsai, S.-J. Jhuo, and M.-J. Cheng, *Org. Electron.*, **9**, 667 (2008).
6. M. D. Groner, F. H. Fabreguette, J. W. Elam, and S. M. George, *Chem. Mater.*, **16**, 639 (2004).
7. E. Guziewicz, I. A. Kowalik, M. Godlewski, K. Kopalko, V. Osinniy, A. Wójcik, S. Yatsunenko, E. Łusakowska, W. Paszkowicz, and M. Guziewicz, *J. Appl. Phys.*, **103**, 033515 (2008).
8. D. M. King, X. Liang, P. Li, and A. W. Weimer, *Thin Solid Films*, **516**, 8517 (2008).
9. D. H. Levy, D. Freeman, S. F. Nelson, P. J. Cowdery-Corvan, and L. M. Irving, *Appl. Phys. Lett.*, **92**, 192101 (2008).
10. S. Bang, S. Lee, S. Jeon, S. Kwon, W. Jeong, H. Kim, I. Shin, H. J. Chang, H. Park, and H. Jeon, *Semicond. Sci. Technol.*, **24**, 025008 (2009).
11. J. W. Maes, Y. J. Kim, H. S. Park, B. Milligan, and S. Marcus, Personal communication.
12. R. Matero, M. Ritala, M. Leskelä, T. Salo, J. Aromaa, and O. Forsén, *J. Phys. IV*, **9**, Pr8: 493 (1999).
13. M. D. Groner, F. H. Fabreguette, J. W. Elam, and S. M. George, *Thin Solid Films*, **413**, 186 (2002).
14. C. X. Shan, X. Hou, and K.-L. Choy, *Surf. Coat. Technol.*, **202**, 2399 (2008).
15. E. Langereis, M. Bouman, J. Keijmel, S. B. S. Heil, M. C. M. van de Sanden, and W. M. M. Kessels, *ECS Trans.*, **16**(4), 247 (2008).
16. E. Langereis, J. Keijmel, M. C. M. van de Sanden, and W. M. M. Kessels, *Appl. Phys. Lett.*, **92**, 231904 (2008).
17. G. Dingemans, P. Engelhart, R. Seguin, F. Einsele, B. Hoex, M. C. M. van de Sanden, and W. M. M. Kessels, *J. Appl. Phys.*, **106**, 114907 (2009).
18. J. Aarik, A. Aidla, T. Uustare, and V. Sammelselg, *J. Cryst. Growth*, **148**, 268 (1995).
19. J. Aarik, A. Aidla, H. Mändar, and V. Sammelselg, *J. Cryst. Growth*, **220**, 531 (2000).
20. S. B. S. Heil, E. Langereis, F. Roozeboom, M. C. M. van de Sanden, and W. M. M. Kessels, *J. Electrochem. Soc.*, **153**, G956 (2006).
21. J. L. van Hemmen, S. B. S. Heil, J. H. Klootwijk, F. Roozeboom, C. J. Hodson, M. C. M. van de Sanden, and W. M. M. Kessels, *J. Electrochem. Soc.*, **154**, G165 (2007).
22. S. B. S. Heil, J. L. van Hemmen, M. C. M. van de Sanden, and W. M. M. Kessels, *J. Appl. Phys.*, **103**, 103302 (2008).
23. A. Niskanen, K. Arstila, M. Ritala, and M. Leskelä, *J. Electrochem. Soc.*, **152**, F90 (2005).
24. J. Hämäläinen, F. Munnik, M. Ritala, and M. Leskelä, *Chem. Mater.*, **20**, 6840 (2008).
25. H. C. M. Knoops, A. J. M. Mackus, M. E. Donders, M. C. M. van de Sanden, P. H. L. Notten, and W. M. M. Kessels, *Electrochem. Solid-State Lett.*, **12**, G34 (2009).
26. W. M. M. Kessels, S. B. S. Heil, E. Langereis, J. L. van Hemmen, H. C. M. Knoops, W. Keuning, and M. C. M. van de Sanden, *ECS Trans.*, **3**(15), 183 (2007).
27. S. B. S. Heil, F. Roozeboom, M. C. M. van de Sanden, and W. M. M. Kessels, *J. Vac. Sci. Technol. A*, **26**, 472 (2008).
28. E. Langereis, S. B. S. Heil, H. C. M. Knoops, W. Keuning, M. C. M. van de Sanden, and W. M. M. Kessels, *J. Phys. D*, **42**, 073001 (2009).
29. R. Matero, A. Rahtu, M. Ritala, M. Leskelä, and T. Sajavaara, *Thin Solid Films*, **368**, 1 (2000).
30. S. K. Kim, S. W. Lee, C. S. Hwang, Y.-S. Min, J. Y. Won, and J. Jong, *J. Electrochem. Soc.*, **153**, F69 (2006).
31. J. Kwon, M. Dai, M. D. Halls, and Y. J. Chabal, *Chem. Mater.*, **20**, 3248 (2008).
32. D. M. Goldstein, J. A. McCormick, and S. M. George, *J. Phys. Chem. C*, **112**, 19530 (2008).
33. D. R. Lide, *CRC Handbook of Chemistry and Physics*, 89th ed., CRC Press, Boca Raton (2009).
34. D. M. King, X. Du, A. S. Cavanagh, and A. W. Weimer, *Nanotechnology*, **19**,

445401 (2008).
35. M. Ritala, M. Leskelä, L. Niinistö, and P. Haussalo, *Chem. Mater.*, **5**, 1174 (1993).
36. A. Rahtu and M. Ritala, *Chem. Vap. Deposition*, **8**, 21 (2002).
37. X. Liang, D. M. King, P. Li, and A. W. Weimer, *J. Am. Ceram. Soc.*, **92**, 649 (2009).
38. E. Langereis, W. Keuning, S. Rushworth, A. Kingsley, F. Roozeboom, M. C. M. van de Sanden, and W. M. M. Kessels, in *Proceedings of the 9th International Conference on Atomic Layer Deposition*, American Vacuum Society, p. 3248 (2009).
39. N. Blasco, R. Katamreddy, Z. Wang, V. Omarjee, P. Venkateswara Rao, and C. Dussarrat, Personal communication.
40. R. Katamreddy, Z. Wang, V. Omarjee, P. Venkateswara Rao, C. Dussarrat, and N. Blasco, *ECS Trans.*, **25**(4), 217 (2009).
41. K.-E. Elers, T. Blomberg, M. Peussa, B. Aitchison, S. Haukka, and S. Marcus, *Chem. Vap. Deposition*, **12**, 13 (2006).
42. K. Kukli, J. Aarik, A. Aidla, O. Kohan, T. Uustare, and V. Sammelselg, *Thin Solid Films*, **260**, 135 (1995).
43. J. Aarik, A. Aidla, K. Kukli, and T. Uustare, *J. Cryst. Growth*, **144**, 116 (1994).
44. C. H. An and K. Sugimoto, *J. Electrochem. Soc.*, **139**, 1956 (1992).
45. W. J. Maeng and H. Kim, *Electrochem. Solid-State Lett.*, **9**, G191 (2006).
46. W. J. Maeng, S.-J. Park, and H. Kim, *J. Vac. Sci. Technol. B*, **24**, 2276 (2006).
47. M. Hellwig, A. Milanov, D. Barreca, J.-L. Deborde, R. Thomas, M. Winter, U. Kunze, R. A. Fischer, and A. Devi, *Chem. Mater.*, **19**, 6077 (2007).
48. S. K. Kim and C. S. Hwang, *J. Appl. Phys.*, **96**, 2323 (2004).